

# Supporting Information

# A high-performance H<sub>2</sub> gas sensor based on PtO<sub>x</sub> and PdO<sub>y</sub> co-decorating WO<sub>3</sub> film

Yongqi Yang,<sup>a</sup> Huaian Fu,<sup>a</sup> Fei Song,<sup>a</sup> Shanshan Yu,<sup>a</sup> Zhipeng Tang,<sup>a</sup> Kai Zhang,<sup>a</sup> Qiuxia Li,<sup>a</sup> Chen Yang,<sup>a</sup> Lixin Zhang,<sup>a</sup> Jinshun Wang,<sup>a</sup> Yuhao Pang,<sup>a</sup> Cao Wang,<sup>a\*</sup> Jingwei Chen,<sup>a\*</sup> Qiang Jing<sup>a\*</sup> and Bo Liu<sup>a\*</sup>

<sup>a</sup>Laboratory of Functional Molecules and Materials, School of Physics and Optoelec-tronic Engineering, Shandong University of Technology, 266 Xincun Xi Road, Zibo, 255000, China

\*Corresponding author(s).

E-mail(s): wangcao@sdut.edu.cn; chenjingwei@sdut.edu.cn; jingqiang@sdut.edu.cn; liub@sdut.edu.cn;

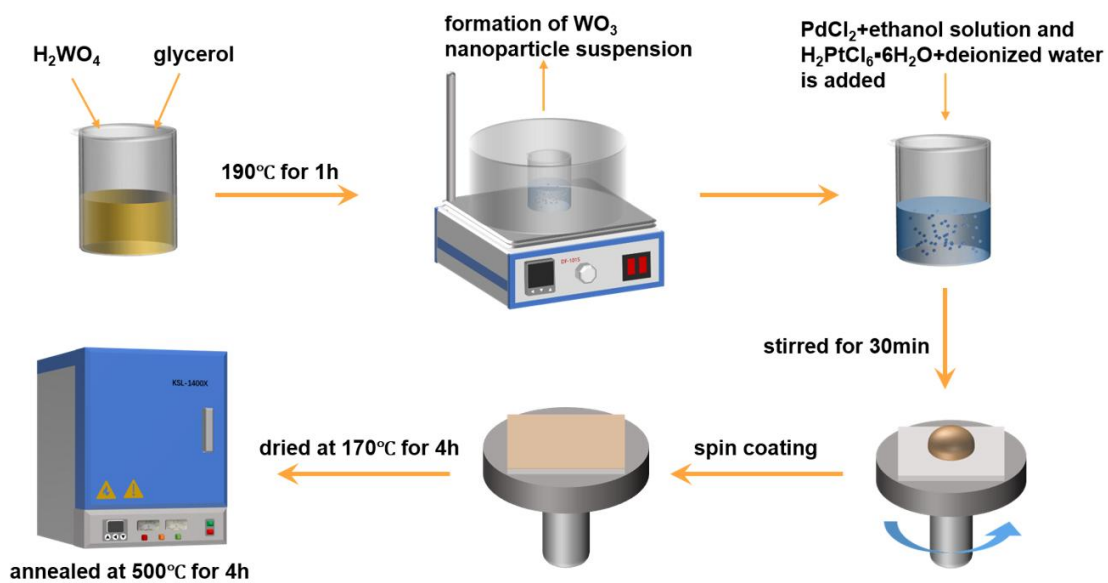


**Fig.S1:** Schematic diagram of the synthesis of the sensing film.

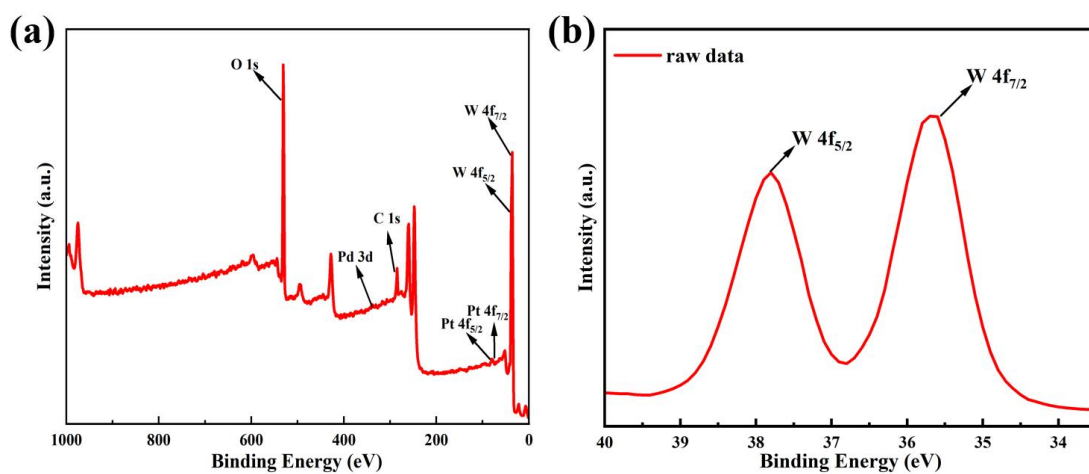


**Fig.S2:** (a) The survey XPS spectrum of the sensing film. (b) The core level spectra of W element.

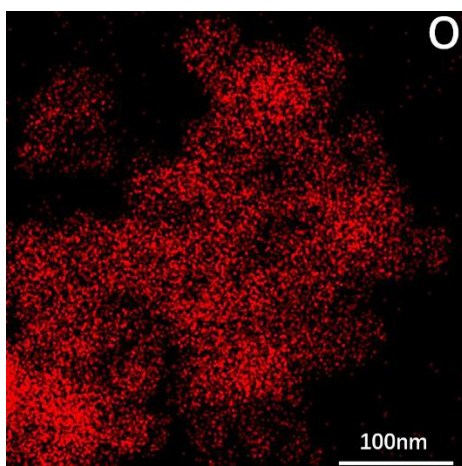


**Fig.S3:** The EDS mapping result of the O element for the sensing film.

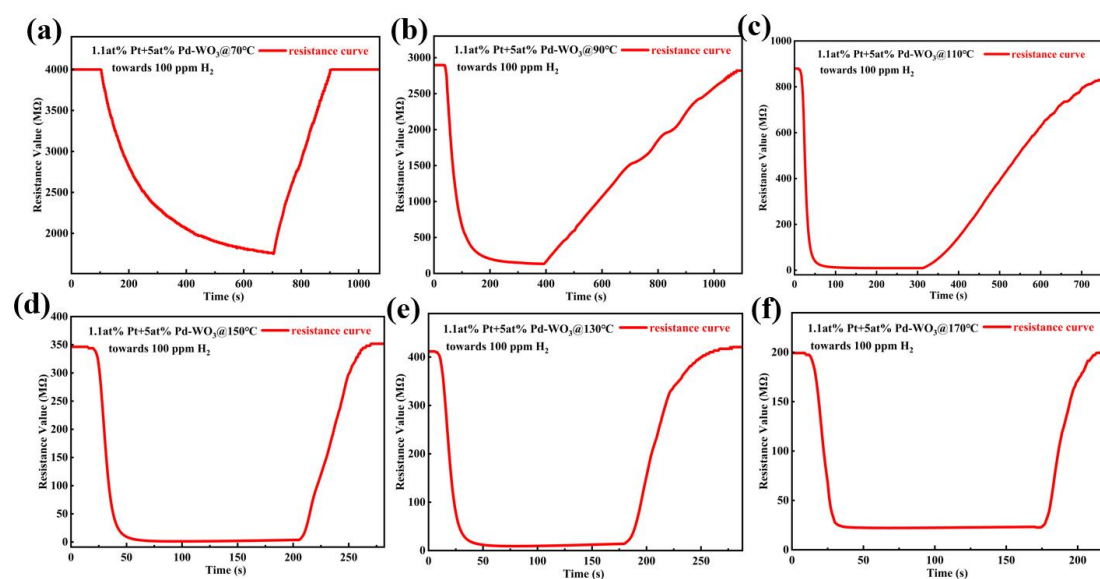


**Fig.S4:** (a)-(f) The real-time resistance variation of the sensor based on 1.1 at% Pt and 5 at% Pd decorating  $\text{WO}_3$  film towards 100 ppm  $\text{H}_2$ , tested at 70, 90, 110, 130, 150 and 170 °C, respectively.

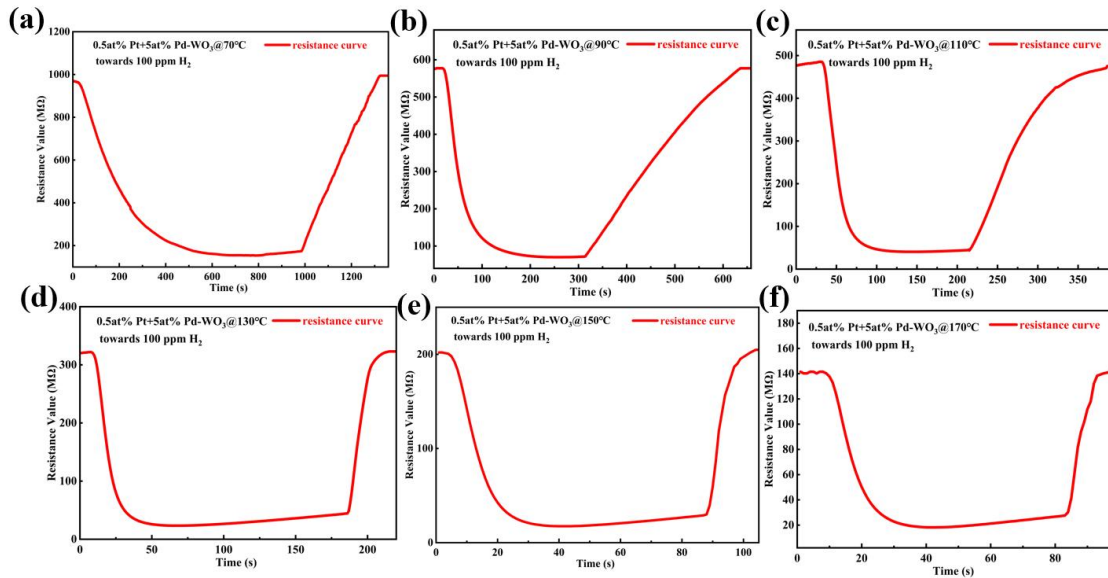


**Fig.S5:** (a)-(f) The real-time resistance variation of the sensor based on 0.5 at% Pt and 5 at% Pd decorating  $\text{WO}_3$  film towards 100 ppm  $\text{H}_2$ , tested at 70, 90, 110, 130, 150 and 170 °C, respectively.

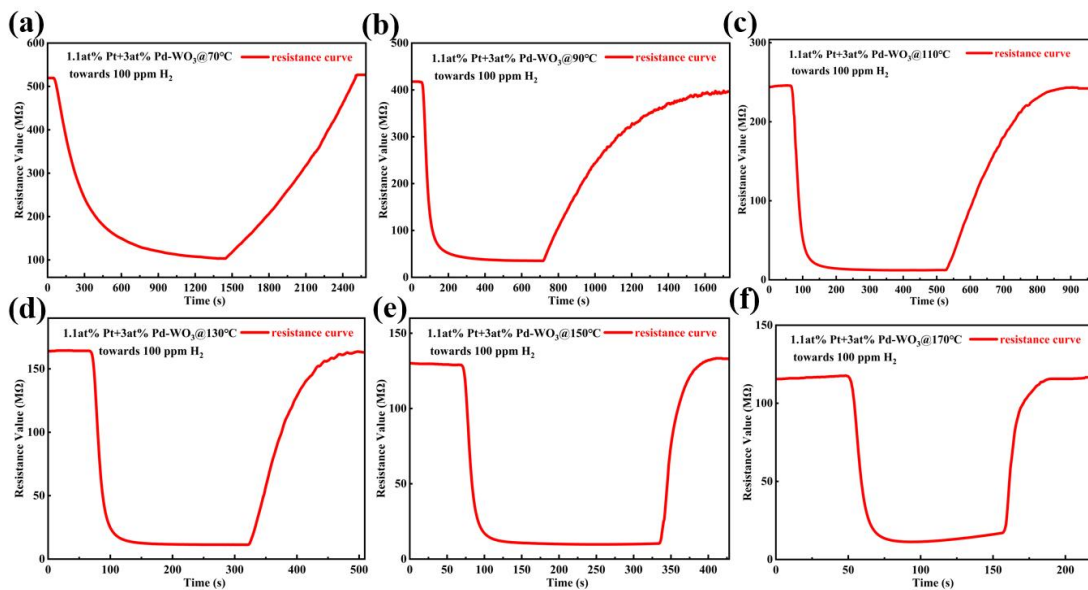


**Fig.S6:** (a)-(f) The real-time resistance variation of the sensor based on 1.1 at% Pt and 3 at% Pd decorating  $\text{WO}_3$  film towards 100 ppm  $\text{H}_2$ , tested at 70, 90, 110, 130, 150 and 170 °C, respectively.

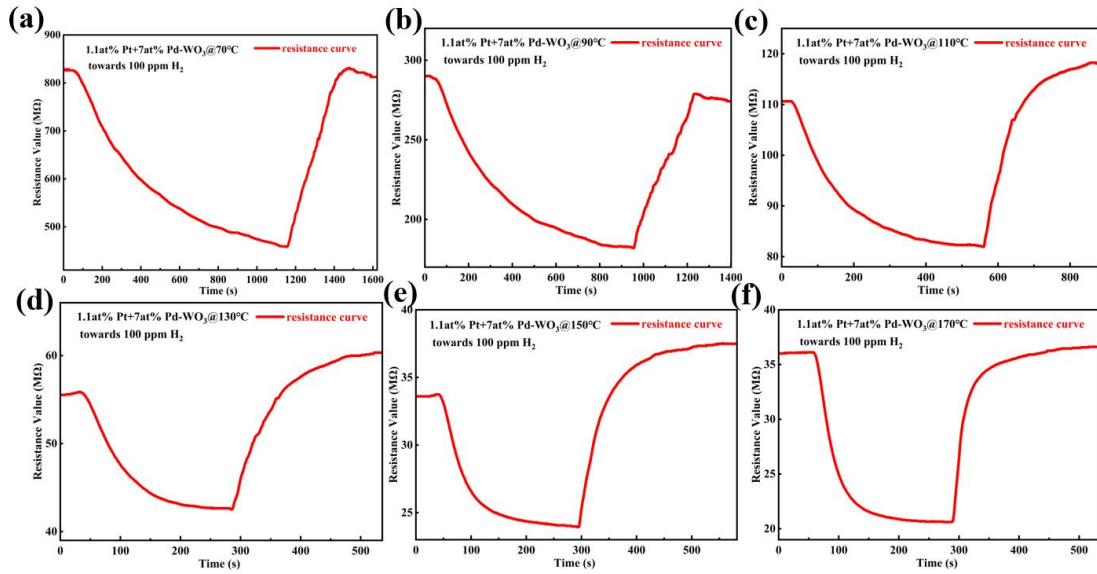


**Fig.S7:** (a)-(f) The real-time resistance variation of the sensor based on 1.1 at% Pt and 7 at% Pd decorating  $\text{WO}_3$  film towards 100 ppm  $\text{H}_2$ , tested at 70, 90, 110, 130, 150 and 170 °C, respectively.

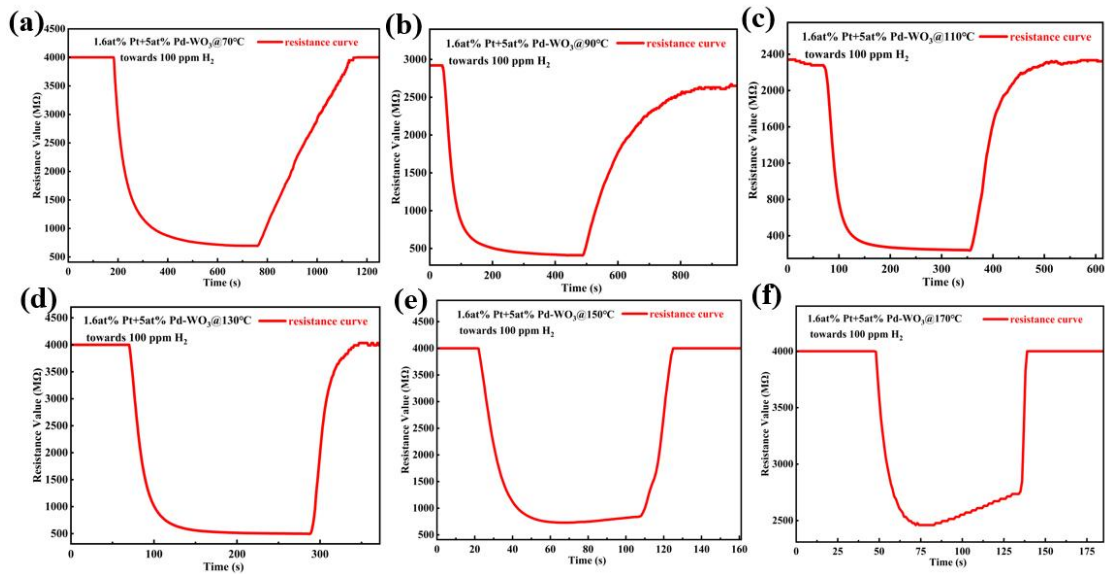


**Fig.S8:** (a)-(f) The real-time resistance variation of the sensor based on 1.6 at% Pt and 5 at% Pd decorating  $\text{WO}_3$  film towards 100 ppm  $\text{H}_2$ , tested at 70, 90, 110, 130, 150 and 170 °C, respectively.

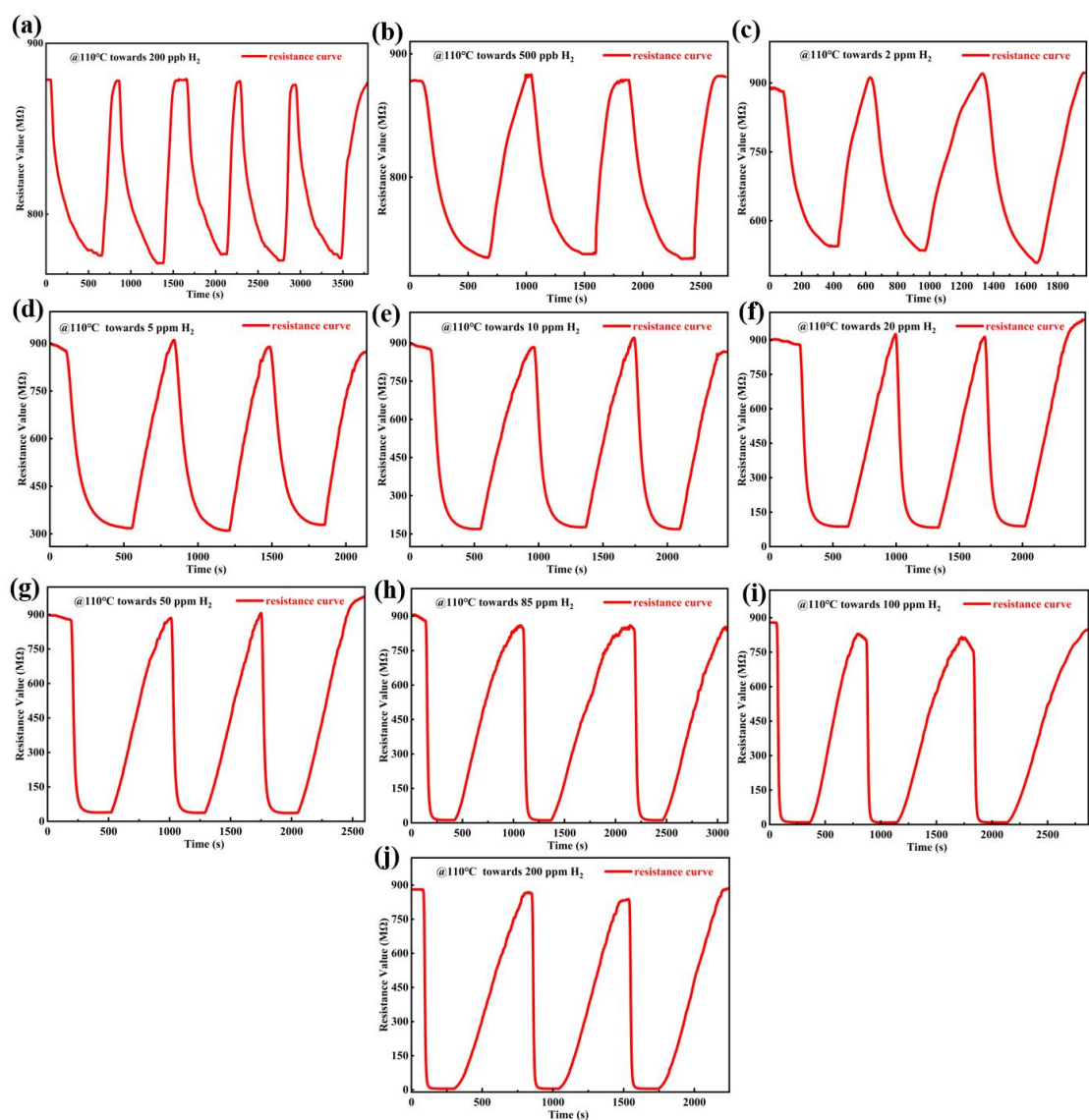


**Fig.S9:** (a)-(j) Repeatability test of Sensor B based on 1.1 at% Pt and 5 at% Pd decorating  $\text{WO}_3$  film for drawing error bars towards 200 ppb-200 ppm  $\text{H}_2$ .

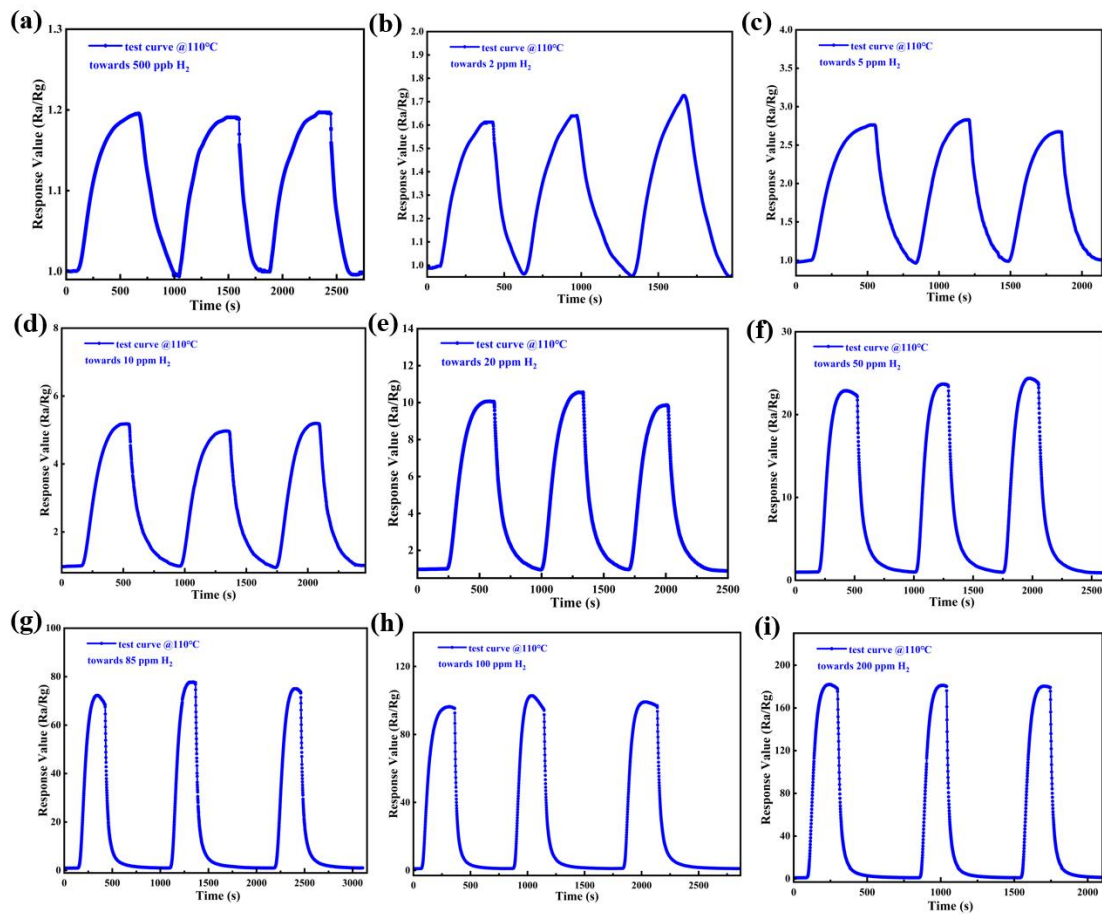


**Fig.S10:** (a)-(i) Reproducibility of the sensor's response to different concentrations of H<sub>2</sub> in order to draw the error bars.



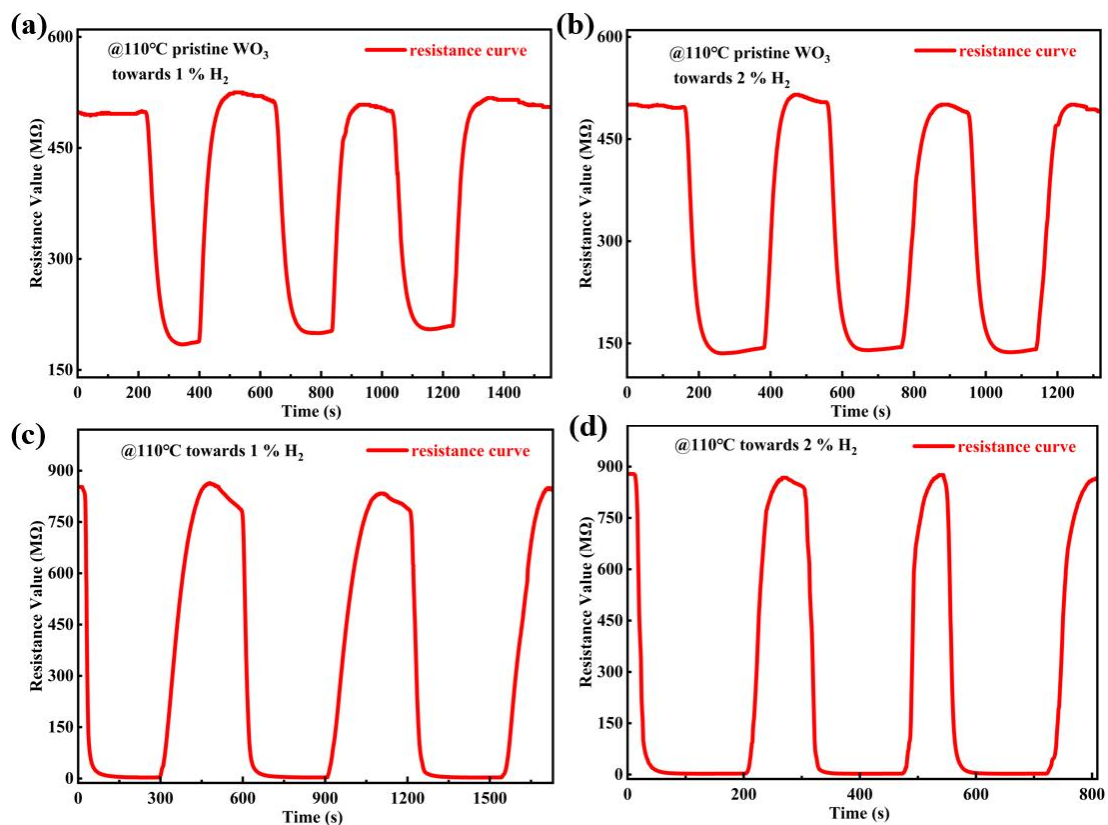


**Fig.S11:** (a)-(b) The real-time resistance of pure WO<sub>3</sub> film to high concentrations of H<sub>2</sub> at 1% and 2%. (c)-(d) The real-time resistance of Sensor B to high concentrations of H<sub>2</sub> at 1% and 2%.

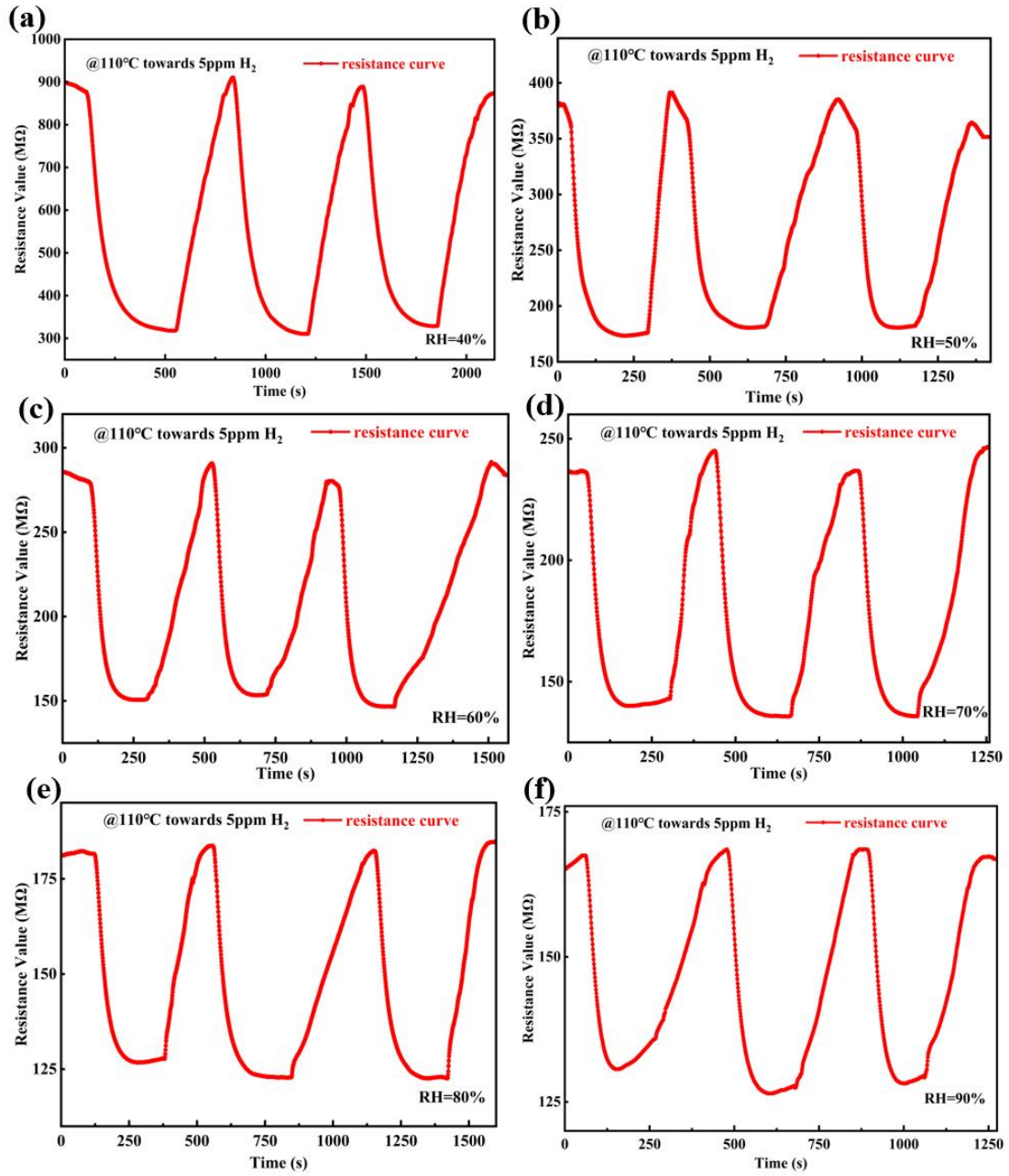
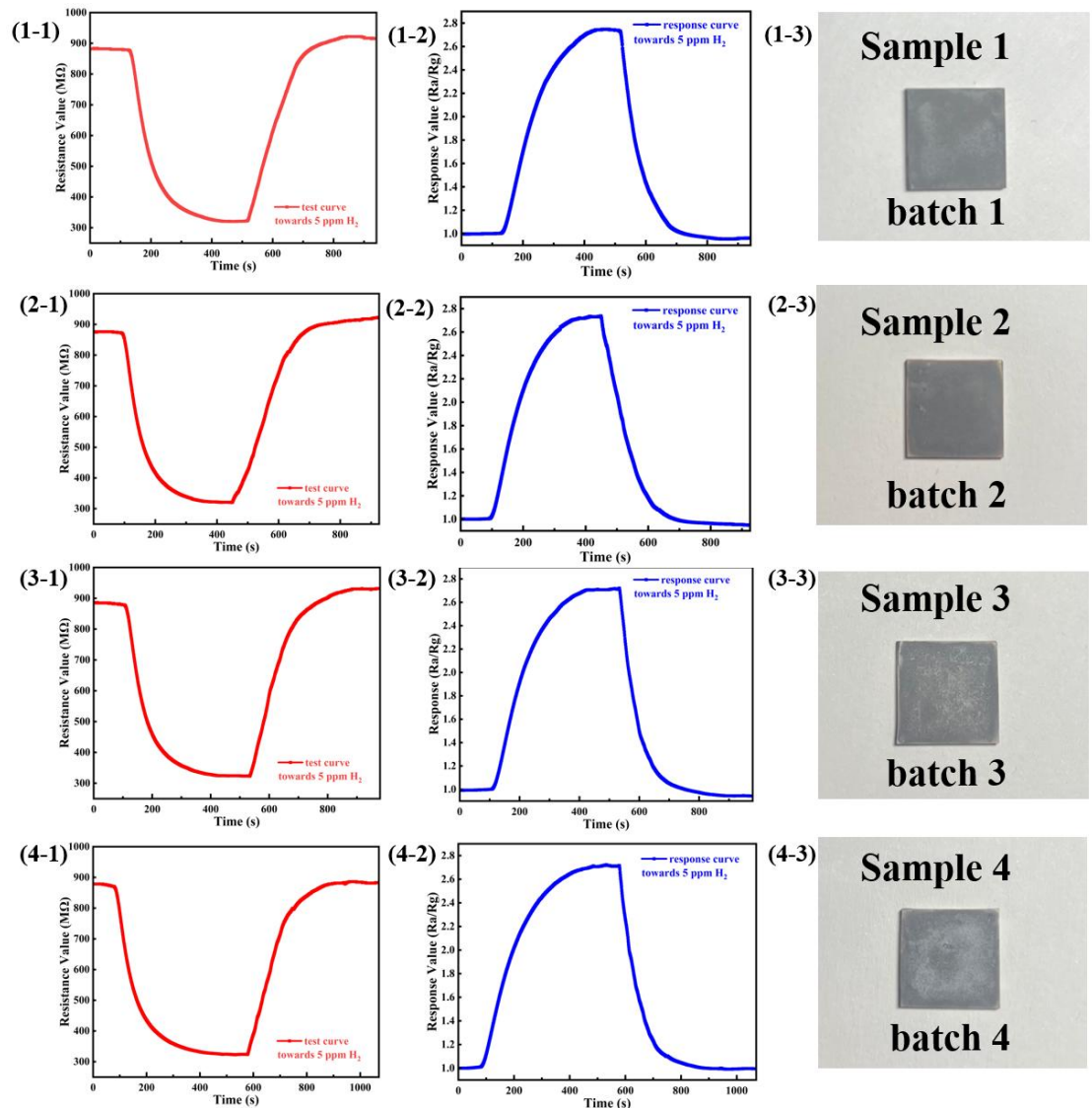
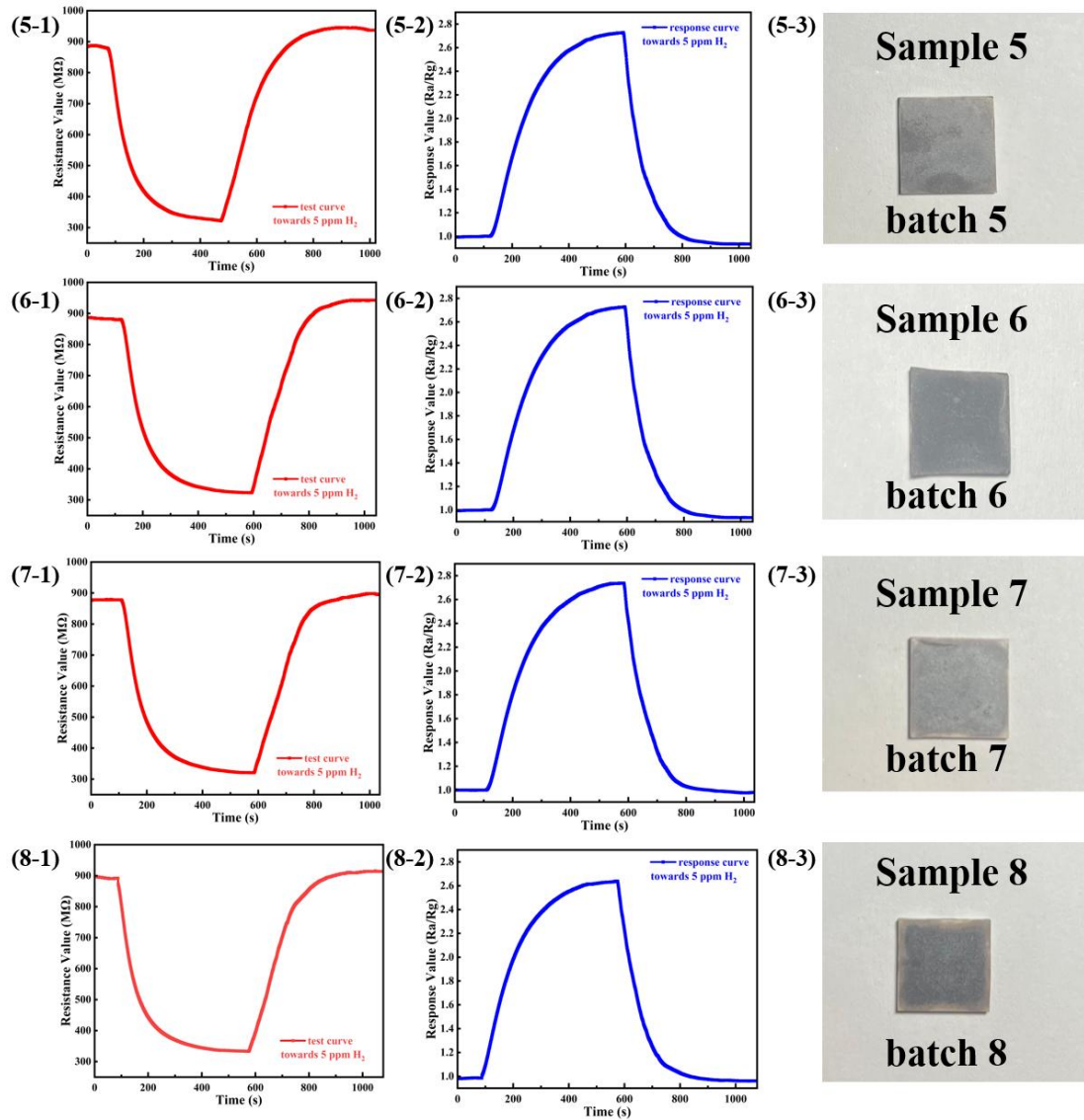


Fig.S12: (a)-(f) The influence of humidity on the response of Sensor B.



**Fig.S13:** (1-1) The real-time resistance variation of Sensor 1 toward 5 ppm H<sub>2</sub>, at 110 °C. (1-2) The response curve corresponding to (1-1). (1-3) The photograph of Sensor 1. (2-1)-(4-3) are the same.



**Fig.S14:** (5-1) The real-time resistance variation of Sensor 5 toward 5 ppm H<sub>2</sub>, at 110 °C. (5-2) The response curve corresponding to (5-1). (5-3) The photograph of Sensor 5. (6-1)-(8-3) are the same.

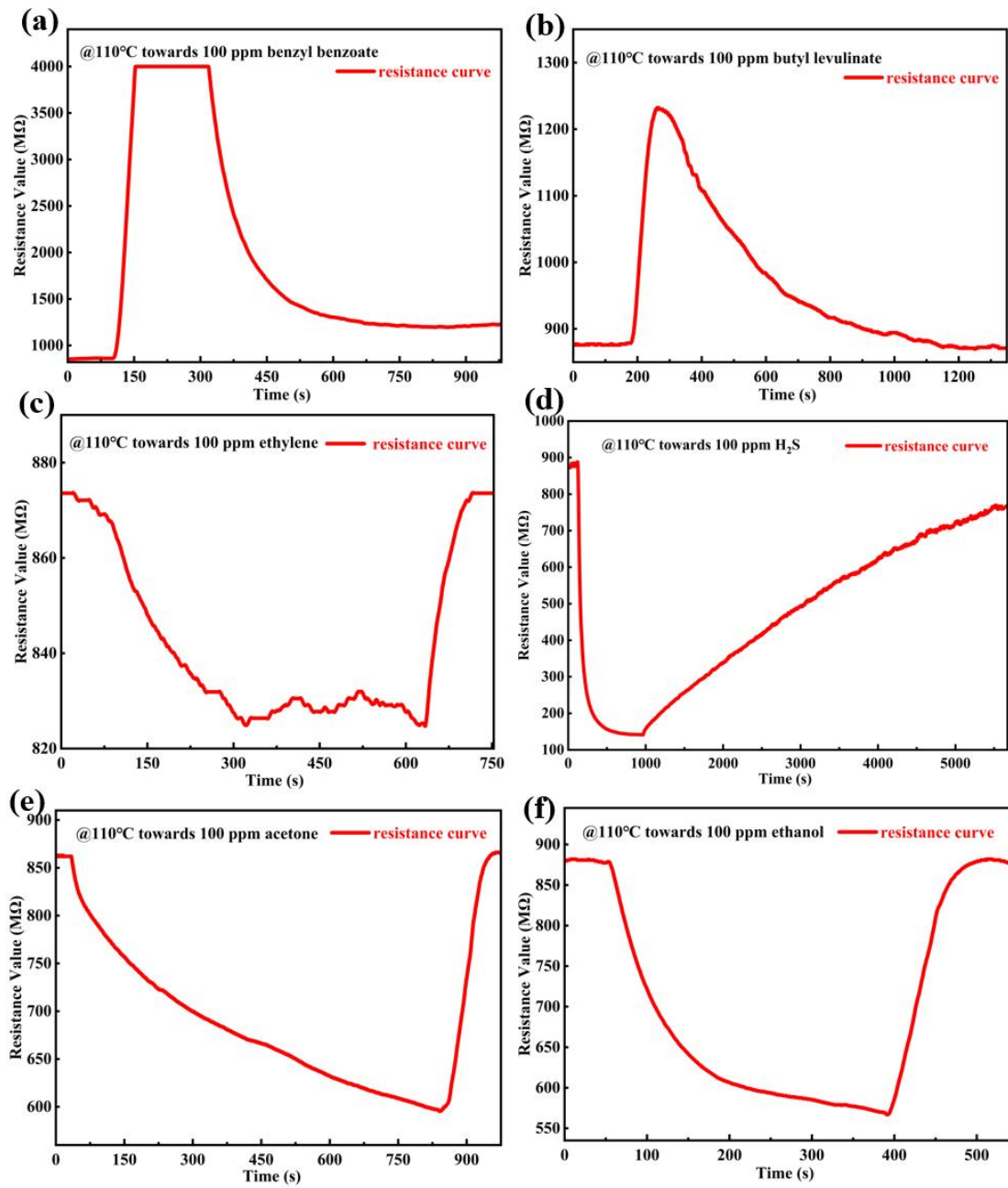


**Fig.S15:** (a)-(f) The selectivity test of Sensor B towards reference gases.

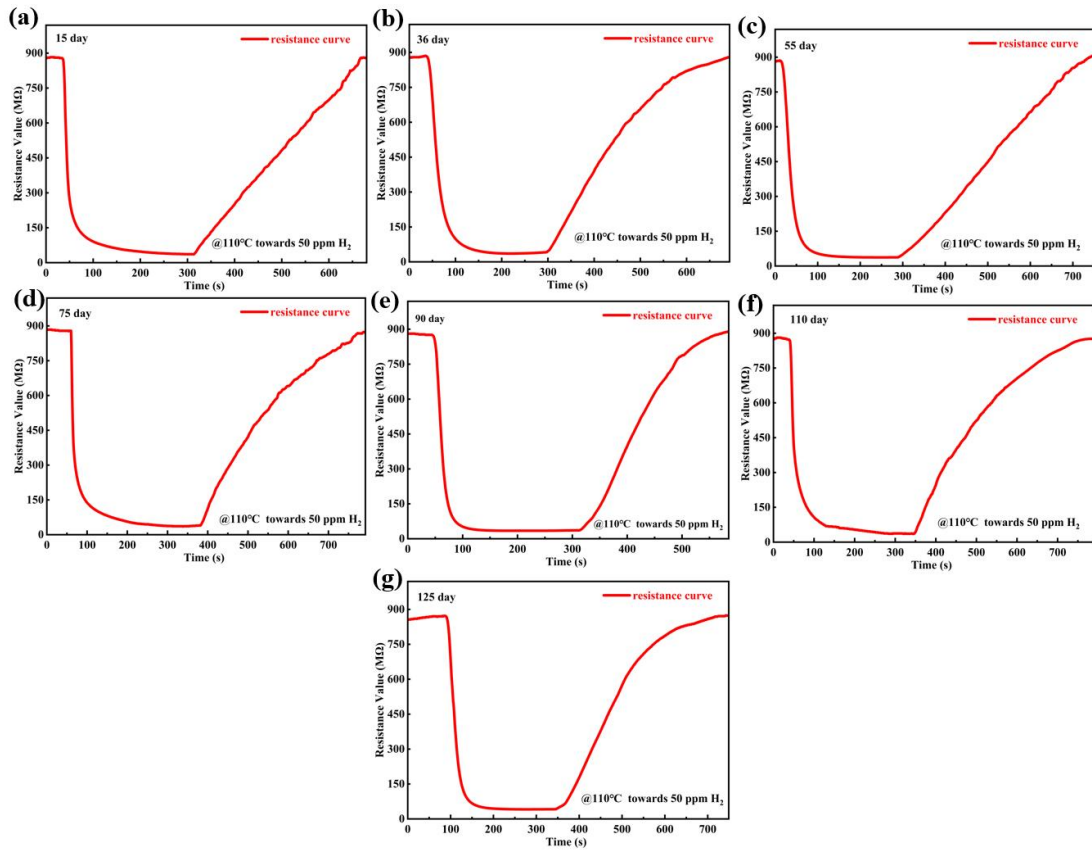


**Fig.S16:** (a)-(g) The long-term stability test of Sensor B.